Geol. Mag. **141** (*1*), *2004, pp. 55–62.* © *2004 Cambridge University Press*
DOI: 10.1017/S0016756803008331 *Printed in the United Kingdom*

Highly heterogeneous Late Mesozoic lithospheric mantle beneath the North China Craton: evidence from Sr–Nd–Pb isotopic systematics of mafic igneous rocks

ZHANG HONG-FU*†, SUN MIN‡, ZHOU MEI-FU‡, FAN WEI-MING*, ZHOU XIN-HUA* & ZHAI MING-GUO*

*Laboratory of Lithosphere Tectonic Evolution, Institute of Geology and Geophysics, Chinese Academy of Sciences, P.O. Box 9825, Beijing 100029, P.R. China
‡Department of Earth Sciences, The University of Hong Kong, Pokfulam Road, Hong Kong

(*Received* 6 February 2003; *accepted* 12 August 2003)

Abstract – The lithospheric mantle beneath the North China Craton changed dramatically in its geophysical and geochemical characteristics from Palaeozoic to Cenozoic times. This study uses samples of Mesozoic basalts and mafic intrusions from the North China Craton to investigate the nature of this mantle in Mesozoic times. Sr–Nd–Pb isotopic data demonstrate that the Late Mesozoic lithospheric mantle was extremely heterogeneous. In the central craton or the Luzhong region, it is slightly Sr–Nd isotopically enriched, beneath the Taihangshan region it has an EM1 character ($^{87}Sr/^{86}Sr_i = 0.7050–0.7066$; $\varepsilon_{Nd(t)} = -17– -10$), and beneath the Luxi–Jiaodong region, it possesses EM2-like characteristics ($^{87}Sr/^{86}Sr_i$ up to 0.7114). Compositional variation with time is also apparent in the Mesozoic lithospheric mantle. Our data suggest that the old lithospheric mantle was modified during Mesozoic times by a silicic melt, where beneath the Luxi–Jiaodong region it was severely modified, but in the Luzhong and Taihangshan regions the effects were much less marked. The silicic melt may have been the product of partial melting of crustal materials brought into the mantle by the subducted slab during the formation of circum-cratonic orogenic belts. This Mesozoic mantle did not survive for a long time, and was replaced by a Cenozoic mantle with depleted geochemical characteristics.

Keywords: Mesozoic, continental lithosphere, isotopes, heterogeneity, silicate melts.

1. Introduction

The lithospheric mantle beneath the North China Craton has a unique evolution from a cold and thick (up to 200 km) Palaeozoic lithosphere (Griffin, O'Reilly & Ryan, 1992; Menzies, Fan & Zhang, 1993) to a hot and thin (< 80 km) Cenozoic lithosphere (Fan *et al.* 2000). This implies a removal of more than 120 km thickness of lithospheric mantle in the Mesozoic. Such a dramatic change has been noted by earlier studies, but the mechanisms responsible for it remain unsolved and contentious. Menzies, Fan & Zhang (1993) suggested that subduction of the Pacific Plate was a driving force to destabilize the cratonic lithosphere. Zheng (1999) and Zheng *et al.* (2001) proposed that the old lithospheric keel was replaced by young oceanic lithosphere. Xu *et al.* (1998) and Xu (2001) emphasized the importance of a thermo-mechanical erosion from the base of the lithosphere. On the basis of Mesozoic basin development of the North China Craton, Menzies & Xu (1998) argued that thermal and chemical erosion in the Jurassic would have been triggered by circum-craton subduction and subsequent continental extension. However, more geochemical data are needed to test these suggestions.

Mesozoic mantle-derived magmatic rocks in the North China Craton potentially provide constraints on the mantle evolution in the region and rigorously test the above models. This paper reports the results of a Sr–Nd–Pb isotopic study on Mesozoic basalts, gabbros and mafic dykes of the North China Craton in order to constrain the evolution of Mesozoic lithospheric mantle beneath the North China Craton. We will also discuss a possible mechanism responsible for such an evolution.

2. Geological background and petrology

The North China Craton consists of two Archaean blocks, the eastern and western blocks, separated by a Palaeoproterozoic orogenic belt (Zhao *et al.* 2001). The basement of the Archaean blocks consists predominantly of Archaean to Proterozoic tonalite–trondhjemite–granodiorite (TTG) gneisses and green-schist to granulite facies, metamorphic rocks, covered by Sinian to Ordovician marine carbonates and shales. Carboniferous to Permian continental clastic rocks, and Mesozoic basin deposits. Mesozoic mafic rocks are

† Author for correspondence: hfzhang@mail.igcas.ac.cn

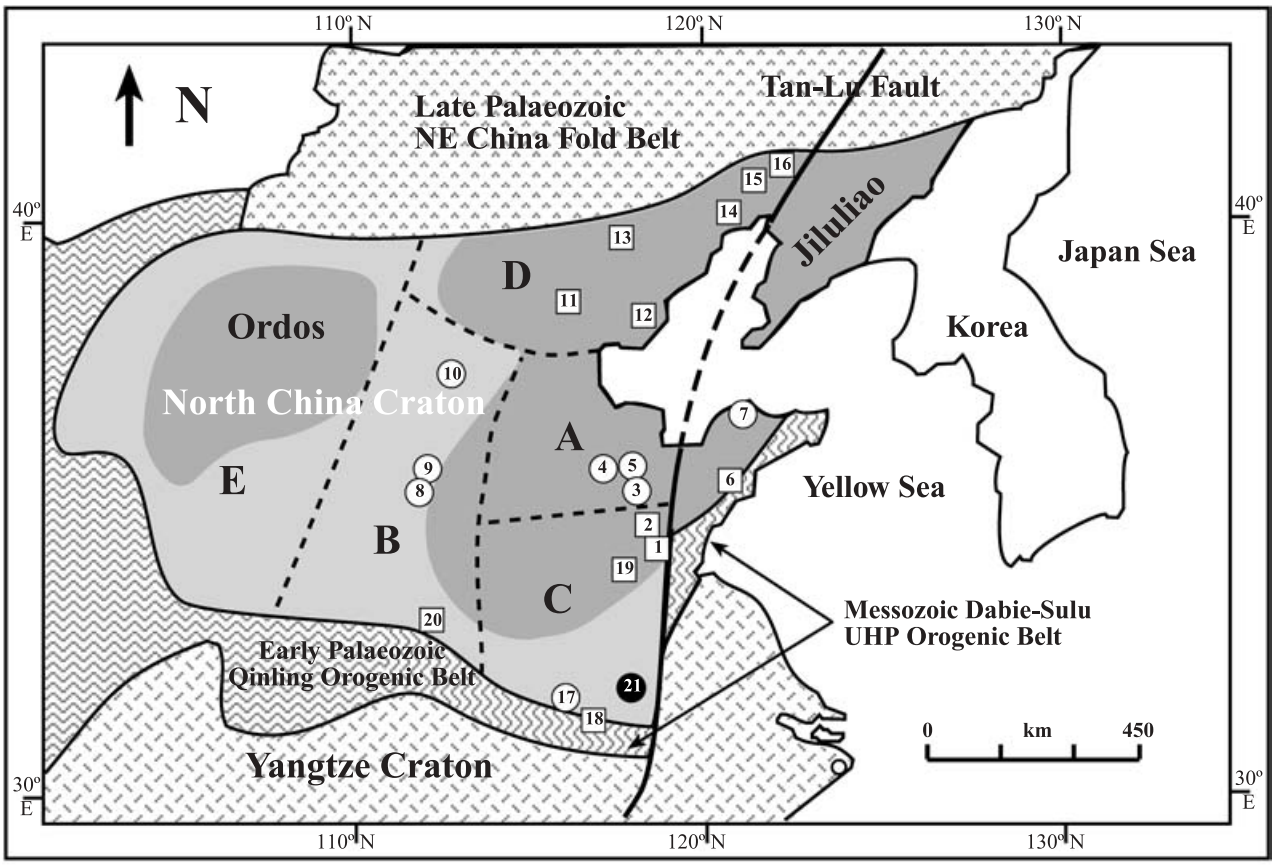

Figure 1. Simplified tectonic map showing major tectonic units in eastern China and localities of Mesozoic basaltic fields and mafic intrusions on the North China Craton (modified from Fan *et al.* 2000). Two Archaean nuclei in the North China craton, Ordos in the west and Jiluliao in the east, were separated by the Palaeoproterozoic orogenic belt. Basaltic fields (open squares) or mafic intrusions (open circles): 1 – Fangcheng basalt; 2 – Mengyin shoshonite; 3 – Laiwu gabbro-diorite complex; 4 – Jinan gabbro; 5 – Zouping gabbro-diorite complex; 6 – Jimo basalt; 7 – Jiaodong mafic dykes; 8 – Donggang gabbro; 9 – Guyi and Fushan gabbros; 10 – Laiyuan gabbro-pyroxenite complex; 11–16 – Western Beijing, Jianchang, Chifeng, Yixian, Fuxin, Zhangwu basalts; 17 – North Huaiyang basaltic rocks; 18 – Northern Dabie gabbro-pyroxenite complex; 19 – Tongshi syenite; 20 – Xinyang xenolith-bearing ultramafic volcanic pipe; 21 – Early Tertiary basalt in Hefei basin. Mesozoic lithospheric mantle blocks: A – Luzhong slightly enriched mantle; B – Taihangshan EM1 mantle; C – Luxi–Jiaodong EM2-like mantle; D – Northern margin 'mixed' mantle; E – Ordos old cratonic mantle. Dashed line shows the possible boundary between the different isotopic regions.

widespread and show the following spatial distribution: mafic volcanism occurs in small extensional basins, dominantly in the Luxi–Jiaodong region and along the northern margin of the North China Craton (Fig. 1), whereas mafic intrusions crop out in the Taihangshan and Luzhong regions (Fig. 1). Volcanic rocks predominantly erupted in early Cretaceous times (Table 1), while the gabbroic intrusions in the Taihangshan region have Jurassic ages (Table 1).

Mafic volcanic rocks include Fangcheng basalts (Zhang *et al.* 2002), Mengyin shoshonites (Qiu, Xu & Lo, 2002), Jimo basalts (Fan *et al.* 2001) and Liaoxi basalts (Chen *et al.* 1997; Zhang *et al.* 2003) (Fig. 1). All these rocks fall in the calc-alkaline series and are rich in Si, Ca, Mg, K, Na and LILE (large ion lithophile elements), and depleted in HFSEs (high field strength elements), a feature similar to island-arc volcanic rocks. Mafic intrusions such as the Jinan gabbros (Guo *et al.* 2001), Zouping and Laiwu gabbro-diorite complexes (L. H. Chen, unpub. Ph.D. thesis, Chinese Acad. Sciences, 2001), and Hanxing and Laiyuan gabbro-monzonite/pyroxenite complexes (Tan & Lin, 1994) are also calc-alkaline (Fig. 1). All the mafic intrusions show quite similar chemical characteristics. Some of them contain peridotite and/or pyroxenite xenoliths (Xu, Zheng & Wang, 1999; L. H. Chen, unpub. Ph.D. thesis, Chinese Acad. Sciences, 2001). Previous petrological and geochemical studies (Tan & Lin, 1994; L. H. Chen, unpub. Ph.D. thesis, Chinese Acad. Sciences, 2001) indicate that the gabbroic bodies did not undergo extensive fractional crystallization but have compositions of original basaltic magmas. Therefore, isotopic features of these mafic rocks could reflect the nature of their mantle source.

3. Analytical procedures

Fresh rock samples were ground with an agate mill and powders were spiked with mixed isotope tracers,

Table 1. Eruption and emplacement age of mafic rocks in eastern North China Craton

District	Rock type	Age (Ma)	Method	Data source
Centre of the North China Craton, Luzhong Region				
Jinan	Gabbro	115	WR Ar–Ar	Lin, Tan & Jing, 1996
Zouping	Gabbro[a]	120 ± 5	Strata	Guo *et al.* 2001
Laiwu	Gabbro[a]	125	WR K–Ar	L. H. Chen, unpub. Ph.D. thesis, Chinese Acad. Sciences, 2001
Taihangshan Region				
Hanxing	Gabbro[a]	150–160	WR K–Ar	This study; Tan & Lin, 1994
Laiyuan	Gabbro[a]	135–145	WR K–Ar	This study
Luxi–Jiaodong Region				
Fangcheng	Basalt	125	WR K–Ar	Zhang *et al.* 2002
Mengyin	Shoshonite	115–124	WR Ar–Ar	Qiu, Xu & Lo, 2002
Jimo	Basalt	110–130	WR K–Ar	Fan *et al.* 2001
Jiaodong	Mafic dyke	120–130	WR K–Ar	J. H. Yang, unpub. Ph.D. thesis, Chinese Acad. Sciences, 2000
Northern margin of the North China Craton				
Fuxin City	Basalt	96–110	WR K–Ar	Zhu, unpub. data
Fuxin County	Basaltic	134–142	WR K–Ar	Zhang *et al.* 2003
Yixian	Basalt[b]	131.2 ± 3	WR Ar–Ar	Chen *et al.* 1997; Wang, Hu & Li, 2001
Yixian	Basalt[c]	120–124	WR K–Ar	Zhu, unpub. data
Chifeng	Basalt	94–107	WR K–Ar	Zhang *et al.* 2003

a – Age determined from the diorite in the gabbro-diorite complex; b – Basalt from the base of the Yixian Formation; c – Basalt from the upper section of the Yixian Formation. WR – Whole rock.

dissolved in Teflon capsules with $HF + HNO_3$ acid, and separated by conventional cation-exchange techniques. The isotopic measurements were performed on a VG-354 mass-spectrometer at the Institute of Geology and Geophysics, Chinese Academy of Sciences. The mass fractionation corrections for Sr and Nd isotopic ratios were based on $^{86}Sr/^{88}Sr = 0.1194$ and $^{146}Nd/^{144}Nd = 0.7219$. Repeat analyses yielded a $^{87}Sr/^{86}Sr$ ratio of 0.71023 ± 0.00006 for the NBS-987 Sr standard and a $^{143}Nd/^{144}Nd$ ratio of 0.511845 ± 0.000012 for the La Jolla standard.

For Pb isotope determinations, 200 mg of powder were weighed into a Teflon vial, spiked and dissolved in concentrated HF at 80 °C for 72 hours. Pb was separated and purified by conventional cation-exchange techniques (AG1 × 8, 200–400 resin) with diluted HBr as an eluant. Isotopic ratios were measured with the VG-354 mass-spectrometer at the Institute of Geology and Geophysics. Repeat analyses of NBS981 yielded $^{204}Pb/^{206}Pb = 0.05897 \pm 15$, $^{207}Pb/^{206}Pb = 0.91445 \pm 80$, $^{208}Pb/^{206}Pb = 2.16170 \pm 180$. Detailed descriptions of the analytical techniques are given elsewhere (Zhang *et al.* 2002, and references therein). All analytical results in this study are presented in Tables 2 and 3.

4. Results

Mafic rocks from the North China Craton show a large variation in isotopic composition ($^{87}Sr/^{86}Sr_i = 0.7034 - 0.7114$; $\varepsilon_{Nd(t)} = -21$–$5$; $^{206}Pb/^{204}Pb_i = 16.4 - 18.2$; $\Delta 8/4 = -30$–130; see Table 3). They also display a clear regional variation, especially in Sr–Nd isotopic composition (Fig. 2). Gabbros from the Taihangshan region have relatively restricted Sr and Nd isotopic ratios ($^{87}Sr/^{86}Sr_i = 0.7050 - 0.7066$; $\varepsilon_{Nd(t)} = -17$–$-10$), typical of the EM1 signature. In contrast, basalts and mafic dykes from the Luxi–Jiaodong region have extremely high $^{87}Sr/^{86}Sr_i$ ratios (up to 0.7114) with Nd isotope compositions similar to those of the Taihangshan mafic intrusions, and are EM2-like (Fig. 2). This EM2-like isotopic signature observed in these rocks from the Luxi–Jiaodong region is also the feature for the gabbros and pyroxenites from the Northern Dabie area (Fig. 2). The latter was interpreted to have been derived from the mantle source that was severely affected by crust-mantle interaction during deep subduction (Jahn *et al.* 1999).

In the Luzhong region, the majority of gabbros have similar $^{87}Sr/^{86}Sr_i$ ratios, but higher ε_{Nd} values ($^{87}Sr/^{86}Sr_i = 0.7045 - 0.7065$; $\varepsilon_{Nd(t)} = -10$–$-4$), relative to those gabbros from the Taihangshan region. A few gabbros from the Luzhong region have very low $^{143}Nd/^{144}Nd$ isotopic ratios ($\varepsilon_{Nd(t)} < -15$), but their Sr isotopic compositions are similar to the rest. Basalts from the northern margin of the North China Craton exhibit large Sr and Nd isotopic variations (Fig. 2); they plot overwhelmingly within the mantle array ($^{87}Sr/^{86}Sr_i = 0.7034 - 0.7066$; $\varepsilon_{Nd(t)} = -9$–5). All the mafic rocks (basalts and gabbros) from the Luxi–Jiaodong, Luzhong and Taihangshan regions have similar Pb isotopic compositions (Table 3, Fig. 3), that is, low $^{206}Pb/^{204}Pb_i$ ratios (< 17.6) and high $\Delta 8/4$ (> 50), different from basalts from the northern margin, which predominantly show higher $^{206}Pb/^{204}Pb_i$ ratios (> 17.5) and low $\Delta 8/4$ values (-30–60) (Fig. 3).

Table 2. Sr–Nd isotopic ratios of Mesozoic mafic rocks

Sample	Rb (ppm)	Sr (ppm)	$^{87}Rb/^{86}Sr$	$^{87}Sr/^{86}Sr$	$(^{87}Sr/^{86}Sr)_i$	Sm (ppm)	Nd (ppm)	$^{147}Sm/^{144}Nd$	$^{143}Nd/^{144}Nd$	$(^{143}Nd/^{144}Nd)_i$	$\varepsilon_{Nd(t)}$
Luzhong region: Jinan gabbro (t = 115 Ma)											
JN2	18.07	515.6	0.1013	0.704876	0.704710	2.20	9.06	0.1468	0.512266	0.512156	−6.5
JN4	29.70	615.1	0.1396	0.704865	0.704637	3.04	12.58	0.1461	0.512288	0.512178	−6.1
JN14	12.28	563.9	0.0630	0.704793	0.704690	2.69	10.87	0.1496	0.512233	0.512120	−7.2
JN6	19.00	433.5	0.1267	0.705416	0.705209	3.82	14.87	0.1553	0.512262	0.512145	−6.7
JN7	33.00	421.1	0.2266	0.705676	0.705306	2.38	14.67	0.0981	0.512208	0.512134	−6.9
JN8-1	25.16	425.7	0.1709	0.705486	0.705207	3.15	15.66	0.1216	0.512367	0.512276	−4.2
JN9	14.18	436.3	0.0940	0.705506	0.705352	3.21	15.34	0.1265	0.512201	0.512106	−7.5
JN10	24.08	427.4	0.1629	0.705357	0.705091	3.89	13.86	0.1697	0.512231	0.512103	−7.5
JN13	20.39	498.6	0.1182	0.705676	0.705483	2.76	12.88	0.1295	0.512199	0.512102	−7.6
Taihangshan region: Guyi and Fushan gabbro (t = 155 Ma)											
FS10	6.14	715.1	0.0248	0.706452	0.706397	3.89	18.26	0.1288	0.511726	0.511595	−16.5
HXY3	31.86	727.4	0.1266	0.706453	0.706174	4.94	22.88	0.1305	0.511904	0.511772	−13.0
HXY6	36.26	875.2	0.1198	0.706716	0.706452	6.10	29.14	0.1265	0.511840	0.511712	−14.2
HXY7	35.17	871.5	0.1167	0.706621	0.706364	5.83	28.23	0.1248	0.511850	0.511723	−14.0
GY1	9.73	956.1	0.0294	0.706677	0.706612	5.57	25.57	0.1317	0.511922	0.511788	−12.7
GY2	13.13	256.4	0.1480	0.706272	0.705946	4.35	18.72	0.1405	0.511942	0.511800	−12.5
GY3	12.80	252.7	0.1464	0.706383	0.706060	4.14	19.22	0.1302	0.511936	0.511804	−12.4
Taihangshan region: Donggang gabbro (t = 155 Ma)											
DG1	35.52	649.2	0.1582	0.705447	0.705098	3.74	18.18	0.1244	0.511906	0.511780	−12.9
DG2	36.42	592.4	0.1777	0.705527	0.705135	4.28	21.40	0.1209	0.511804	0.511681	−14.8
DG3	31.26	640.0	0.1412	0.705169	0.704858	3.83	17.51	0.1322	0.511883	0.511749	−13.5
DG4	28.61	657.3	0.1258	0.705191	0.704914	3.62	16.86	0.1298	0.511900	0.511768	−13.1
Taihangshan region: Laiyuan gabbro (t = 140 Ma)											
WLG-01	30.01	398.7	0.2176	0.706486	0.706053	3.40	15.33	0.1342	0.511965	0.511842	−12.0
WLG-02	25.67	729.0	0.1018	0.706101	0.705898	6.08	23.11	0.1590	0.512031	0.511885	−11.2
WLG-03	35.33	699.7	0.1460	0.706283	0.705993	6.75	28.12	0.1451	0.512012	0.511879	−11.3
WLG-04	34.17	854.4	0.1156	0.706280	0.706050	2.27	9.67	0.1418	0.511959	0.511829	−12.3
WLG-05	45.74	1642	0.0805	0.706219	0.706059	5.13	28.00	0.1109	0.511884	0.511782	−13.2
WLG-06	74.65	1317	0.1638	0.706312	0.705986	3.64	21.78	0.1010	0.511867	0.511775	−13.3
WLG-08	95.40	893.7	0.3086	0.706290	0.705676	5.03	29.43	0.1032	0.511931	0.511836	−12.1
WLG-09	1.72	2330	0.0021	0.705860	0.705856	4.84	19.26	0.1519	0.512038	0.511899	−10.9
LMG-01	11.10	406.6	0.0789	0.706456	0.706299	2.54	13.56	0.1134	0.511743	0.511639	−16.0
LMG-02	18.31	481.0	0.1101	0.706034	0.705815	4.13	18.07	0.1383	0.511747	0.511620	−16.3
LMG-03	16.09	506.6	0.0918	0.706124	0.705941	5.25	23.78	0.1334	0.511776	0.511654	−15.7
LMG-04	9.34	326.7	0.0827	0.705924	0.705759	1.89	9.51	0.1204	0.511745	0.511635	−16.1
LMG-05	11.23	489.6	0.0663	0.706000	0.705868	2.45	12.82	0.1157	0.511733	0.511627	−16.2
LMG-06	9.78	1200	0.0236	0.706024	0.705977	3.22	14.84	0.1313	0.511803	0.511683	−15.1
LMG-07	43.28	1718	0.0728	0.705824	0.705679	4.42	21.16	0.1264	0.511782	0.511666	−15.4
LMG-10	46.39	1576	0.0851	0.706235	0.706066	6.22	38.97	0.0965	0.511775	0.511687	−15.0
LMG-11	46.41	1590	0.0844	0.706388	0.706220	5.52	32.68	0.1021	0.511786	0.511692	−14.9
LMG-12	33.87	1558	0.0628	0.705969	0.705844	5.97	36.19	0.0998	0.511797	0.511706	−14.7
LMG-13	40.37	1804	0.0647	0.706284	0.706155	4.71	28.80	0.0988	0.511791	0.511701	−14.8
LMG-14	70.03	1152	0.1757	0.706338	0.705988	4.57	27.86	0.0992	0.511699	0.511608	−16.6

Chondrite Uniform Reservoir (CHUR) values ($^{87}Rb/^{86}Sr = 0.0847$, $^{87}Sr/^{86}Sr = 0.7045$, $^{147}Sm/^{144}Nd = 0.1967$, $^{143}Nd/^{144}Nd = 0.512638$) are used for the initial isotopic ratio calculation.

5. Discussion

5.a. Mantle heterogeneity

The lack of a positive correlation of $^{87}Sr/^{86}Sr_i$ with SiO_2 or Mg no. in these Mesozoic mafic rocks (Fig. 4) suggests that the process of crustal contamination was insignificant in generating the major differences between the different sample groupings. This is further supported by the high MgO contents of these rocks (Fan *et al.* 2001; Guo *et al.* 2001; Zhang *et al.* 2002, 2003). The presence of mantle xenoliths in some basalts and intrusions (Xu, Zheng & Wang, 1999; Zhang *et al.* 2002) also demonstrates that the parental magmas ascended rapidly, which did not allow significant contamination. Therefore, these mafic rocks are taken to reflect the isotopic compositions of the Mesozoic lithospheric mantle beneath the North China Craton. Data from this study demonstrates the extreme heterogeneity and clear regional variation in this mantle. The lithospheric mantle beneath the central North China Craton was slightly Sr–Nd isotopically enriched toward an EM1 component, showing EM1 characteristics beneath the Taihangshan and an EM2-like character under the Luxi–Jiaodong region. In contrast, the lithospheric mantle beneath the northern margin appears to be more complicated: it was generally depleted (DMM) but with some involvement of an EM1 component (Fig. 2). Here, we have applied the following names to these isotopically distinctive regions: Luzhong slightly enriched mantle, Taihangshan EM1 mantle, Luxi–Jiaodong EM2 mantle, and northern margin 'mixed' mantle (Fig. 1). In contrast to the

Table 3. Pb isotopic ratios of Mesozoic mafic rocks

Sample	$^{206}Pb/^{204}Pb$	$^{207}Pb/^{204}Pb$	$^{208}Pb/^{204}Pb$	$^{238}U/^{204}Pb$	$^{206}Pb/^{204}Pb_i$	$^{207}Pb/^{204}Pb_i$	$^{208}Pb/^{204}Pb_i$	Δ7/4	Δ8/4
Luzhong region: Jinan gabbro (t = 115 Ma)									
JN2	16.626	15.226	36.456	3.6685	16.560	15.223	36.369	−6.3	72.2
JN4	16.910	15.220	36.587	4.6363	16.827	15.216	36.477	−9.9	50.7
JN14	16.827	15.266	36.734	0.4644	16.819	15.266	36.724	−4.8	76.3
JN6	16.939	15.288	36.692	5.6669	16.837	15.283	36.586	−3.3	60.4
JN7	16.735	15.269	36.408	5.0007	16.645	15.265	36.290	−3.0	54.0
JN8-1	16.743	15.269	36.518	2.7323	16.694	15.266	36.379	−3.4	56.9
JN9	16.828	15.272	36.599	3.2051	16.771	15.269	36.505	−4.0	60.2
JN10	16.744	15.264	36.472	4.1713	16.669	15.260	36.378	−3.9	59.9
JN13	16.701	15.248	36.454	3.3802	16.640	15.245	36.374	−5.0	62.9
Taihangshan region: Guyi and Fushan gabbro (t = 155 Ma)									
FS10	16.968	15.210	37.039	6.2490	16.816	15.203	36.791	−11.1	83.4
HXY3	17.416	15.257	38.007	1.1529	17.388	15.256	37.964	−12.0	131.5
HXY6	17.193	15.180	37.731	1.0245	17.168	15.179	37.691	−17.3	130.6
HXY7	17.160	15.223	37.661	0.5850	17.146	15.223	37.632	−12.7	127.6
Taihangshan region: Donggang gabbro (t = 155 Ma)									
GY1	17.474	15.250	37.614	11.5638	17.192	15.237	37.246	−11.8	83.4
GY2	18.063	15.308	39.180	12.1116	17.768	15.293	38.072	−12.4	96.3
GY3	17.605	15.243	38.058	6.9072	17.437	15.235	37.262	−14.6	55.3
DG1	17.236	15.257	37.529	6.9183	17.068	15.249	37.336	−9.3	107.4
DG2	17.022	15.273	36.934	6.5121	16.863	15.265	36.709	−5.4	69.5
DG3	17.154	15.273	37.379	3.9239	17.058	15.268	37.236	−7.2	98.5
DG4	17.083	15.295	37.261	3.8168	16.990	15.290	37.170	−4.3	100.2
Taihangshan region: Laiyuan gabbro (t = 140 Ma)									
WLG-01	16.928	15.265	36.982	6.023	16.795	15.259	36.839	−5.3	90.7
WLG-02	16.635	15.182	36.493	2.602	16.578	15.179	36.454	−10.9	78.4
WLG-03	16.743	15.283	36.846	3.046	16.676	15.280	36.765	−1.9	97.8
WLG-04	16.729	15.249	36.745	1.512	16.695	15.247	36.716	−5.3	90.4
WLG-06	16.719	15.233	36.743	5.442	16.600	15.228	36.611	−6.3	91.5
WLG-08	16.867	15.219	36.726	6.778	16.719	15.212	36.530	−9.1	69.0
WLG-09	16.678	15.254	36.643	1.116	16.653	15.253	36.624	−4.3	86.3
LMG-01	16.693	15.203	36.866	4.347	16.598	15.199	36.706	−9.1	101.2
LMG-02	16.802	15.200	36.748	7.735	16.632	15.192	36.426	−10.2	69.1
LMG-03	16.681	15.089	36.444	2.013	16.636	15.087	36.361	−20.8	62.0
LMG-04	16.786	15.219	36.666	2.725	16.726	15.216	36.579	−8.8	73.0
LMG-06	16.641	15.194	36.689	1.682	16.604	15.192	36.635	−9.9	93.4
LMG-07	16.659	15.173	36.918	2.511	16.604	15.170	36.848	−12.1	114.7
LMG-10	16.863	15.284	36.973	6.039	16.730	15.277	36.802	−2.7	94.8
LMG-11	16.774	15.260	36.808	6.907	16.623	15.253	36.627	−4.0	90.3
LMG-12	17.031	15.218	37.511	4.328	16.936	15.213	37.388	−11.4	128.5
LMG-13	16.825	15.282	36.921	6.776	16.676	15.275	36.713	−2.4	92.4
LMG-14	16.579	15.228	37.106	3.103	16.510	15.225	36.910	−5.6	132.2

$\Delta 7/4 = [(^{207}Pb/^{204}Pb)_i - (^{207}Pb/^{204}Pb)_{NHRL}] \times 100$; $\Delta 8/4 = [(^{208}Pb/^{204}Pb)_i - (^{208}Pb/^{204}Pb)_{NHRL}] \times 100$; $(^{207}Pb/^{204}Pb)_{NHRL} = 0.1084 \times (^{206}Pb/^{204}Pb)_i + 13.491$; $(^{208}Pb/^{204}Pb)_{NHRL} = 1.209 \times (^{206}Pb/^{204}Pb)_i + 15.627$.

above regions in the eastern block, the western block does not show significant magmatism after Palaeozoic times (Fig. 1). Therefore, Mesozoic lithospheric mantle beneath the western block may be quite different, that is, it has inherited characteristics from the old and cold lithosphere.

5.b. Temporal–spatial evolution

The present data clearly show a spatial evolutionary trend for the Mesozoic lithospheric mantle, that is, a gradual trend towards the more radiogenic in the Sr isotopic ratio and the less radiogenic in the Nd isotopic ratio from the centre of the North China Craton (block A in Fig. 1) to the Luxi–Jiaodong (block C) and Taihangshan regions (block B). Interestingly, this mantle also shows pronounced isotopic enrichment with time. In Luxi–Jiaodong region, basaltic rocks have ages from 170 to 120 Ma, and these rocks become more and more enriched in radiogenic Sr isotope compositions (Fig. 5), with the highest $^{87}Sr/^{86}Sr_i$ ratio (0.712) at 120 Ma. Similarly, in the northern margin of the North China Craton, Mesozoic basalts show a similar trend in Nd isotopes with time (see Xu, 2001, fig. 7). We consider that these significant temporal and spatial evolutionary trends were most likely related to a significant tectonic and thermal event in eastern China.

5.c. Origin of mantle enrichment – interaction with silicic melt

Mantle enrichment beneath the North China Craton can be interpreted as resulting from an influx of melts from a subducted continental slab, which over

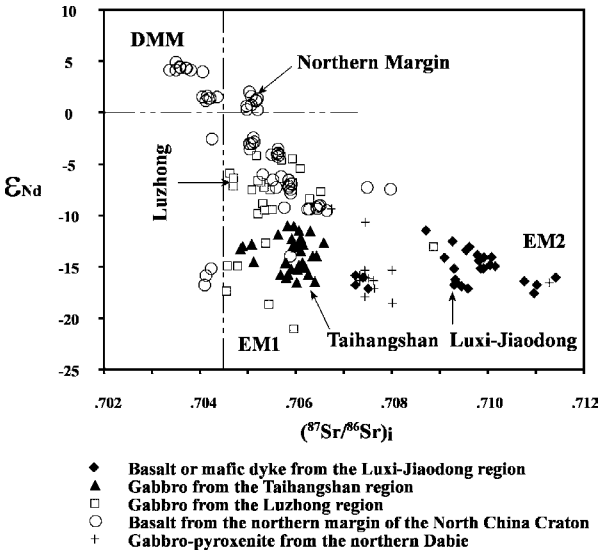

Figure 2. Initial Sr–Nd isotopic diagram for Mesozoic mafic rocks (calculated to the time of Table 1). Data sources are from this study and the literature: Luzhong region (this study, Guo *et al.* 2001; L. H. Chen, unpub. Ph.D. thesis, Chinese Acad. Sciences, 2001); Taihangshan region (this study); Luxi–Jiaodong region (J. H. Yang, unpub. Ph.D. thesis, Chinese Acad. Sciences, 2000; Fan *et al.* 2001; Qiu, Xu & Lo, 2002; Zhang *et al.* 2002); Northern margin of the NCC (Chen *et al.* 1997; Zhang *et al.* 2003); Gabbro-pyroxenite from the Northern Dabie (Li *et al.* 1998; Jahn *et al.* 1999). DMM: depleted MORB (mid-ocean ridge basalt) mantle; EMI – enriched mantle 1; EM2 – enriched mantel 2.

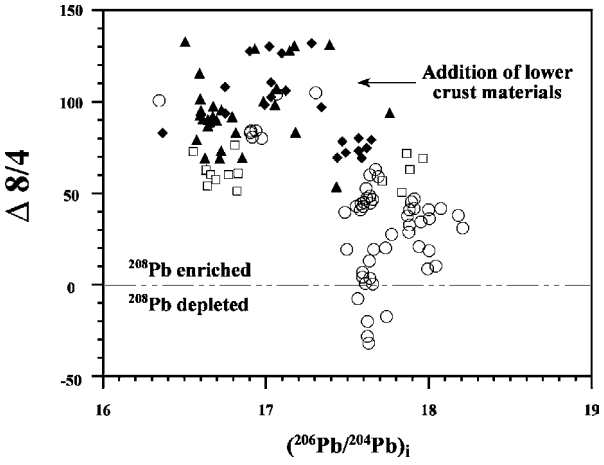

Figure 3. Initial $^{206}Pb/^{204}Pb$ v. $\Delta 8/4$ diagram for the Mesozoic mafic rocks on the NCC. $\Delta 8/4 = [(^{208}Pb/^{204}Pb)_i - (^{208}Pb/^{204}Pb)_{NHRL}] \times 100$; $(^{208}Pb/^{204}Pb)_{NHRL} = 1.209 \times (^{206}Pb/^{204}Pb)_i + 15.627$. $\Delta 8/4 > 0$ indicates the presence of high Th/Pb ratio in the rock, subsequently resulting to the enrichment in the radiogenic ^{208}Pb. Symbols and data sources as in Figure 2.

time would develop isotopic heterogeneity (Zhang & Sun, 2002). This melt was high in the LILEs and radiogenic Sr isotopic compositions, and low in HFSEs and radiogenic Nd–Pb isotopic compositions. Silicic melt with these geochemical characteristics can only be derived by partial melting of an old lower crust.

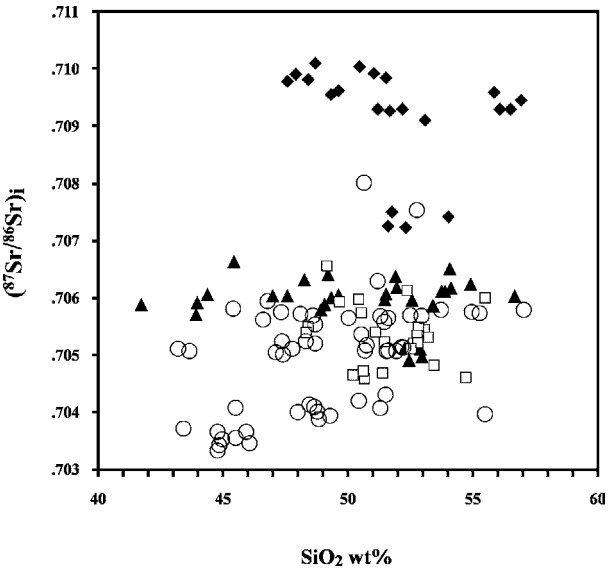

Figure 4. SiO_2 v. $^{87}Sr/^{86}Sr_i$ isotopic ratios for Mesozoic mafic rocks. Symbols and data sources as in Figure 2.

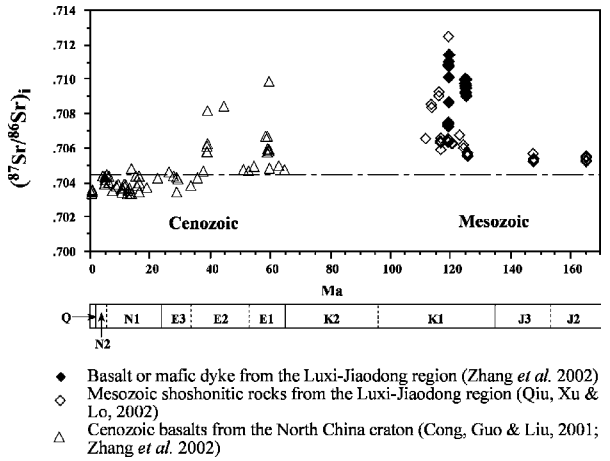

Figure 5. Sr isotopic variation with time in Mesozoic and Cenozoic basalts and shoshonitic rocks.

High Th/U ratios of the rocks in this study (enriched in ^{208}Pb) indicate the possible involvement of middle, even upper crust in their sources.

The Mesozoic lithosphere was undoubtedly evolved from the Palaeozoic lithosphere, thus it should have inherited some Palaeozoic lithosphere signatures. Mantle xenoliths have been discovered in Palaeozoic kimberlites from the North China Craton and these xenoliths have very restricted Nd isotopic compositions ($\varepsilon_{Nd} \simeq -5$: Zhang *et al.* 2002). Nd isotopic compositions for gabbros from the Luzhong region ($\varepsilon_{Nd} < -10$) are slightly lower than those of the Palaeozoic kimberlite-borne mantle xenoliths from the North China Craton, suggesting that their mantle source retained characteristics of the old lithospheric mantle, with slight modification. In contrast, basalts from the Luxi–Jiaodong region have ε_{Nd} values (average ≈ -16, Fig. 2) much lower than those of

the Palaeozoic mantle xenoliths, indicating that the Mesozoic lithospheric mantle beneath the Luxi–Jiaodong region was modified severely by the addition of a significant quantity of silicic melts. The reaction of silicic melts with the refractory Palaeozoic mantle peridotite may have produced pyroxenite veins in the mantle, as evidenced by the occurrence of pyroxenite xenoliths in Fangcheng basalts (Zhang *et al.* 2002). This modified lithosphere (peridotite + pyroxenite) became the source of Mesozoic calc-alkaline basalts and mafic intrusions. The crust-derived silicic melt requires an early subduction process to bring the crust to the mantle depth. Thus, we can envisage that the lithospheric mantle beneath the North China Craton experienced several evolutionary stages during Phanerozoic times, although the subduction could have occurred as early as Palaeozoic times. The Palaeozoic cratonic lithospheric mantle evolved into the Mesozoic enriched lithospheric mantle as a result of interaction with a melt from the subduction of a continental slab. This Mesozoic mantle did not survive for a long time period, since the Cenozoic lithospheric mantle underneath the North China Craton is again very different, that is, it is now fertile but depleted in Sr–Nd isotopic compositions (Fan *et al.* 2000).

6. Conclusions

(1) Mesozoic basalts and mafic intrusions on the North China Craton are largely uncontaminated by continental crust, and therefore can be used to investigate the nature of their mantle sources.

(2) The Mesozoic lithospheric mantle underneath the North China Craton was highly heterogeneous. The mantle beneath the central craton and the Taihangshan region exhibited an EM1 character, that is, it was more enriched in the LREE than Rb, whereas lithospheric mantle beneath the Luxi–Jiaodong region was EM2-like, that is, more enriched in Rb than the LREE.

(3) The Mesozoic lithospheric mantle underneath the North China Craton is envisaged as having evolved from the Palaeozoic mantle severely modified by a silicic melt from a subducted continental slab.

Acknowledgements. This work was funded by Natural Science Foundation of China (40225009), Chinese Academy of Sciences (KZCX1-07, KZCX3-SW-135), HK RGC (HKU7115/00P) and Young Researcher Awards from NSFC and from the University of Hong Kong. R. X. Zhu is thanked for permission to use his unpublished data. We are grateful to M. Menzies for his comments on the earlier version and to B. M. Jahn and J. Baker for their constructive reviews.

References

CHEN, Y. X., CHEN, W. J., ZHOU, X. H., LI, Z. J., LIANG, H. D., LI, Q., XU, K. FAN, Q. C., ZHANG, G. H., WANG, F., WANG, Y., ZHOU, S. Q., CHEN, S. H., HU, B. & WANG, Q. J. 1997. *Liaoxi and adjacent Mesozoic volcanics – chronology, geochemistry and tectonic settings*. Beijing: The Seismological Press, 279 pp. [in Chinese].

CONG, B. L., GUO, J. H. & LIU, W. J. 2001. An ancient mantle wedge: evidence from Early Tertiary volcanics on the North China Craton. *Chinese Science Bulletin* **46**, 1825–30.

FAN, W. M., GUO, F., WANG, Y. J., LIN, G. & ZHANG, M. 2001. Post-orogenic bimodal volcanism along the Sulu orogenic belt in eastern China. *Physics and Chemistry of the Earth (A)* **26**, 733–46.

FAN, W. M., ZHANG, H. F., BAKER, J., JARVIS, K. E., MASON, P. R. D. & MENZIES, M. A. 2000. On and off the North China Craton: where is the Archean keel? *Journal of Petrology* **41**, 933–50.

GRIFFIN, W. L., O'REILLY, S. Y. & RYAN, C. G. 1992. Composition and thermal structure of the lithosphere beneath South Africa, Siberia and China: proton microprobe studies. In *Proceedings, International Symposium on Cenozoic Volcanic Rocks and Deep-seated Xenoliths of China and its Environs*, pp. 1–20. Beijing, August 1992.

GUO, F., FAN, W. M., WANG, Y. G. & LIN, G. 2001. Late Mesozoic mafic intrusive complexes in North China Block: constraints on the nature of subcontinental lithospheric mantle. *Physics and Chemistry of the Earth (A)* **26**, 759–71.

JAHN, B. M., WU, F. Y., LO, C. H. & TSAI, C. H. 1999. Crust-mantle interaction induced by deep subduction of the continental crust: geochemical and Sr–Nd isotopic evidence from post-collisional mafic-ultramafic intrusions of the northern Dabie complex, central China. *Chemical Geology* **157**, 119–46.

LI, S. G., NIE, Y. H., HART, S. R. & ZHENG, S. G. 1998. Upper mantle-deep subducted continental crust interaction: (II) Sr and Nd isotopic constraints on the syn-collisional mafic to ultramafic intrusions in the northern Dabieshan, eastern China. *Science in China (D)* **28**, 18–22.

LIN, J. Q., TAN, D. J. & JINGH, H. 1996. $^{40}Ar/^{39}Ar$ ages for the Mesozoic igneous rocks from the western Shandong Province [in Chinese]. *Journal of Petrology and Mineralogy* **15**(3), 213–19.

MENZIES, M. A., FAN, W. M. & ZHANG, M. 1993. Paleozoic and Cenozoic lithoprobes and the loss of > 120 km of Archean lithosphere, Sino-Korean Craton, China. In *Magmatic Processes and Plate Tectonics* (eds H. M. Pichard, T. Alabaster, N. B. W. Harris and C. R. Neary), pp. 71–8. Geological Society of London, Special Publication no. 76.

MENZIES, M. A. & XU, Y. G. 1998. Geodynamics of the North China Craton. In *Mantle dynamics and plate interactions in East Asia* (eds M. F. J. Flower, A. L. Chung, C. H. Lo and T. Y. Lee), pp. 155–65. American Geophysical Union Monograph no. 27.

QIU, J. S., XU, X. S. & LO, Q. H. 2002. Potassium-rich volcanic rocks and lamprophyres in western Shandong Province: ^{40}Ar–^{39}Ar dating and source tracing. *Chinese Science Bulletin* **47**, 91–9.

TAN, D. J. & LIN, J. Q. 1994. *Mesozoic potassium magma province on North China platform*. Beijing: The Seismological Press, 184 pp. [in Chinese].

WANG, S. S., HU, G. H. & LI, P. X. 2001. The geological age of Yixian Formation in western Liaoning, China. *Bulletin of Mineralogy. Petrology and Geochemistry* **20**, 189–291 [in Chinese with English abstract].

XU, W. L., ZHENG, C. Q. & WANG, D. Y. 1999. The discovery of mantle- and crust-derived xenoliths in

Mesozoic trachybasalts from western Liaoning and their geological implications [in Chinese with English abstract]. *Geological Review* **45**, 444–9.

Xu, Y. G. 2001. Thermo-tectonic destruction of the Archean lithospheric keel beneath the Sino-Korean Craton in China: Evidence, Timing and Mechanism. *Physics and Chemistry of the Earth (A)* **26**, 747–57.

Xu, Y. G., Menzies, M. A., Vroon, P., Mercier, J. C. & Lin, C. Y. 1998. Texture–temperature–geochemistry relationship in the upper mantle as revealed from spinel peridotite xenoliths from Wangqing, NE China. *Journal of Petrology* **39**, 469–93.

Zhang, H.-F. & Sun, M. 2002. Geochemistry of Mesozoic basalts and mafic dikes in southeastern North China craton, and tectonic implication. *International Geology Review* **44**, 370–82.

Zhang, H.-F., Sun, M., Zhou, X. H., Fan, W. M. & Yin, J. F. 2002. Mesozoic lithosphere destruction beneath the North China Craton: evidence from major, trace element, and Sr–Nd–Pb isotope studies of Fangcheng basalts. *Contributions to Mineralogy and Petrology* **144**, 241–53.

Zhang, H.-F., Sun, M., Zhou, X. H., Zhou, M. F., Fan, W. M. & Zheng J. P. 2003. Secular evolution of the lithosphere beneath the eastern North China Craton: evidence from Mesozoic basalts and high-Mg andesites. *Geochimica et Cosmochimica Acta* **67**, 000–000.

Zhao, G. C., Wilde, S. A., Cawood, P. A. & Sun, M. 2001. Archean blocks and their boundaries in the North China Craton: lithological, geochemical, structural and P–T path constraints and tectonic evolution. *Precambrian Research* **107**, 45–73.

Zheng, J. P. 1999. *Mesozoic–Cenozoic mantle replacement and lithospheric thinning, east China*. Wuhan: China University of Geosciences Press, 126 pp. [in Chinese with English abstract].

Zheng, J. P., O'Reilly, S. Y., Griffin, W. L., Lu, F. X., Zhang, M. & Pearson, N. J. 2001. Relict refractory mantle beneath the eastern North China block: significance for lithosphere evolution. *Lithos* **57**, 43–66.